Journal of Nuclear Materials 567 (2022) 153837

Contents lists available at ScienceDirect

Journal of Nuclear Materials

journal homepage: www.elsevier.com/locate/jnucmat

Deuterium retention in the elements of plasma facing components for the DEMO first wall

Y. Gasparyan[a,*], D. Bachurina[a], V. Efimov[a], J. Gurova[a], F. Podolyako[a], N. Sergeev[a,b], I. Sorokin[a,c], A. Suchkov[a], N. Bobyr[b], I. Kozlov[a,d], E. Kulikova[b], A. Spitsyn[a,b]

[a] National Research Nuclear University MEPhI (Moscow Engineering Physics Institute), Kashirskoe shosse 31, 115409 Moscow, Russia
[b] NRC "Kurchatov Institute", Ak. Kurchatov sq., 1, Moscow, 123182, Russia
[c] Kotel'nikov Institute of Radio Engineering and Electronics (Fryazino Branch), Russian Academy of Sciences, Fryazino, Moscow oblast, 141190 Russia
[d] NUST MISIS, 119049 Moscow, Russia

ARTICLE INFO

Article history:
Received 30 December 2021
Revised 25 April 2022
Accepted 1 June 2022
Available online 2 June 2022

ABSTRACT

The fully reduced activation brazing alloy TiZr4Be and a tantalum intermediate layer are considered to be used for joining tungsten (W) to reduced-activation ferritic-martensitic steel (RAFM) for future DEMO reactor application. Deuterium retention in the W-Rusfer joints and separate elements was investigated with the focus on the intermediate brazing layer. The samples were exposed in deuterium gas (p = 1–10^4 Pa, T = 300–600°C) and plasma discharge (T = 600°C). An acceptable deuterium concentration was observed after gas exposure at the pressure of 1 Pa, that is relevant to operating conditions of future fusion devices, however the brazing alloy and tantalum accumulate a large amount of deuterium in the case of the pressure above 100 Pa that leads to failure of the joint. The D retention after D plasma irradiation was substantial, but nearly independent on the fluence and the thickness of the W layer due to absorption from surrounding D_2 gas.

1. Introduction

Due to higher neutron fluxes, fusion power, and operation time in future DEMO reactors in comparison to ITER and current machines, new solutions for plasma facing components (PFC) are under development. One should avoid materials with high induced radioactivity, therefore, reduced-activation ferritic-martensitic steels (RAFM) [1,2] are main candidates for structural materials. Tungsten (W) is one of the most promising PFC materials due to the high thermal conductivity and melting temperature, low sputtering by light plasma particles, low tritium retention and moderate activation by fusion neutrons [3]. Current conceptual designs of DEMO reactors consider tungsten (W) not only for the divertor area, but also for the first wall [4,5]. Due to the difference of thermal expansion coefficients of W and RAFM steels, a direct joining is challenging. Therefore, various intermediate layers (V, Ta, etc.) [6,7] or more complicated concepts with a functionally-graded W-Fe(iron) interlayer [8,9] are proposed. Recently, several interlayer materials and brazing alloys were proposed to join tungsten to steel. The vast majority of investigations is performed with Cu- or Ni-based brazing alloys, which are considered to be highly activated and having low resistance to neutron irradiation [10].

Recently, good mechanical properties of the W-RAFM joint were achieved using Ta as an intermediate layer and the fully reduced activation TiZr4Be brazing alloy [11]. In this work, we investigated the compatibility of this joint with hydrogen gas and plasma exposure since it is unavoidable in fusion devices.

It is known that tantalum, titanium and zirconium can accumulate a large amount of hydrogen with subsequent embrittlement due to hydride formation and fail. However, this problem can be not so pronounced at elevated temperatures and relatively low pressures. The goal of this work was to evaluate acceptable temperatures and hydrogen pressures for safe operation.

2. Experimental details

2.1. Description of initial materials and brazing procedure

The tungsten samples with the size of 5 × 5 × 3 mm^3 (or 5 × 5 × 1 mm^3) were cut from polycrystalline tungsten produced by Polema (Russia) and manufactured according to ITER specifications. The steel samples were cut from EK-181 (Rusfer) (Fe–12Cr–2W–V–Ta–B, wt. %). More information about Rusfer can be found in [12,13]. The sample size was either 5 × 5 × 3 mm^3 or 5 × 10 × 3 mm^3. The steel in its as produced state was used for brazing and in thermal treated state for gas exposure of single materials. Here and after we call steel and tungsten as base materials.

* Corresponding author.
E-mail address: ymgasparyan@mephi.ru (Y. Gasparyan).

https://doi.org/10.1016/j.jnucmat.2022.153837
0022-3115/

The key element of this investigation was the brazing alloy 48Ti-48Zr-4Be wt.% (TiZr4Be) STEMET 1412 rapidly solidified into the ribbon of 70 μm thickness by applying melt spinning technology (see [14] for details). The initial state of the foil was amorphous-crystalline [15]. The same brazing alloy and procedure was also used to braze a self-passivating tungsten alloy to steel [16].

To evaluate the phase composition of the TiZr4Be brazing alloy, synchrotron X-ray diffraction (SynXRD) was used. Before the analysis, the foil was annealed at 600°C for 2 hours that corresponds to the preliminary heating procedure in gas exposure experiments. SynXRD was performed at the X-ray structural analysis beamline of the Kurchatov Synchrotron Radiation Source [17] with 0.74 Å wavelength monochromatic irradiation. A small piece of the foil was placed perpendicular to the beam. The detailed description of the scheme can be found elsewhere [18,19]. The foil was exposed for 240 sec. Indexing of the recorded SynXRD patterns was made using the ICDD PDF4+ database.

Tantalum compensating layers were cut from the 0.2 μm thick foil with the size of 5 × 5 mm.

The brazing of the W/TiZr4Be/Ta/TiZr4Be/Rusfer joint was carried out in a vacuum furnace ($p < 10^{-5}$ mbar). The specimens were fixed by a 200 g load that corresponded to 0.08 MPa. The brazing procedure included thermal heat treatment at 1100°C for 1 hour and aging at 720°C for 3 hours [18]. This treatment corresponds to the heat treatment of Rusfer steel (see details in [20]) and allows to keep its initial properties. Shear strength tests were carried out at room temperature by the scheme presented in [21]. Five samples were measured for each experimental condition. The microstructure of the samples was analyzed using the JEOL JSM-6610LV scanning electron microscope (SEM) with the energy dispersive spectroscopy (EDS) module INCA X-ACT (Oxford Instruments, the U.K.).

Operating conditions for DEMO reactors are not finally defined. The heat and particle fluxes from plasma to PFC can vary during the operation, especially during transient events. There is also internal heating caused by neutron irradiation and further transmutations. According to modeling [22], the steady state heat load to the first wall will be below 1 MW/m^2 in most places, while the peak load of 7 MW/m^2 can be expected at baffle areas. In some PFC designs [23], the temperature of the steel part reaches 523°C already at 0.8 MW/m^2. Independently on the PFC design, the RAFM steels, however, should operate below the critical temperature of 550°C. The temperature at the joining layer is expected to be similar due to its small thickness. Therefore, the temperature of 600°C was taken as a maximal in our experiments.

The typical pressure of hydrogen isotopes during the plasma discharge in ITER is below 1 Pa and the flux of energetic neutrals and charged particles is estimated below 10^{21} particles/m^{2}s [24]. Similar estimates can be expected for DEMO.

2.2. Gas exposure

The exposure of samples in D_2 gas was performed in Kurchatov Institute. For this purpose, a high-vacuum chamber with the volume of 310 cm^3 and the ultimate pressure of $<10^{-6}$ Pa was used. The temperature (T) of the samples was monitored by a type K thermocouple and it was varied from 300 to 600°C. The deuterium pressure (p) during the exposure was measured with a capacitance manometer and it was in the range of 1 – 10^4 Pa. The purity of D_2 gas was above 99,99%. Prior to gas exposure the samples were degassed at 600°C for 2 hours. During exposure, the total gas pressure in the chamber was decreasing due to sorption by samples and it was maintained in the range of ±10%. The exposure time was 50 hours in all experiments. The flux of impurity gases did not exceed 10^{-7} Pa*l/s during the exposure. To avoid a possible contribution in experiments with the lowest gas pressure (1 Pa), the chamber was evacuated continuously during this exposure.

In addition, the annealing of few brazed samples in the initial state was carried out at 600°C for 100 h in argon atmosphere.

2.3. Plasma exposure

Plasma irradiation of the brazed samples was carried out in a linear plasma-chemical reactor based on beam-plasma discharge in MEPhI (see [25] for details). This setup allows to create a stationary plasma with a uniform distribution of electron density and electron temperature in beam cross-section resulting in uniform surface treatment by plasma. Samples were mounted on an electrically insulated holder biased by a DC power supply. During the experiments, only the front tungsten surface of samples was exposed to the plasma beam by using a diaphragm with a diameter of 3 mm mounted in the front of the sample ensuring that only the surface of the sample was interacting with plasma. All plasma irradiation experiments were carried out at the joint point temperature of 600°C, the D_2 pressure of about ~1 Pa, and the sample bias voltage of 300 V. The samples were not actively cooled, and the temperature was controlled by a thermocouple mounted close to the brazed layer. The composition of the ion flux according to the previous studies mainly consists of D_2^+ [25]. Plasma parameters such as plasma density and electron temperature during the exposure were controlled by a single movable Langmuir probe located close to the sample position. *In-situ* ion saturation current measurements with single probe provided incident deuterium ion flux densities of about ~1.2×10^{21} D/m^{2}s in all experiments, but the exposure time was varied from 2 to 16 hours.

2.4. Thermal desorption spectroscopy

The deuterium retention was measured using thermal desorption spectroscopy in the UHV TDS stand in MEPhI (see [25] for details). The heating rate during the TDS analysis was either 0.2 K/s or 2 K/s depending on the expected D amount in the samples. The desorption flux of deuterium-containing masses (D_2, HD, HDO, D_2O) was monitored with the quadrupole mass-spectrometer Pfeiffer Vacuum QME 100 (QMS). The calibration of the absolute sensitivity for D_2 gas was performed after each separate TDS measurement (see [25] for details).

3. Experimental results

3.1. Pre-characterization of materials before deuterium exposure

Fig. 1 presents the SynXRD pattern of the TiZr4Be foil after annealing at 600°C for 2 hours. The foil crystallized completely after annealing (the initial state was amorphous-crystalline [15]) as no amorphous halo is observed in the pattern. Some peaks are overlapped, but we put labels of a phase with the highest intensity above other labels (e.g. β(Ti,Zr) has a higher intensity than Ti_7Zr_3 at 17.5°). The most intense peak at 2θ–18.5° identifies Ti_7Zr_3 compound. This compound was also observed in high-entropy alloy FeMoTaTiZr manufactured by vacuum arc remelting [26]. High temperature solid solution of Ti and Zr (β(Ti,Zr)) and two Be-Zr compounds (Be_2Zr, $Be_{17}Zr_2$) were identified as well. Apart from compounds consisting of alloying elements, there were BeO and ZrO oxides identified. Be and Zr are known for creating a strong chemical bond with oxygen. These oxides were likely formed during casting of the brazing alloy, so they could not be expected to melt during brazing and likely, remained as formed in a brazed seam. Additionally, the oxides were likely to be formed on the surface of the foil during the contact with air.

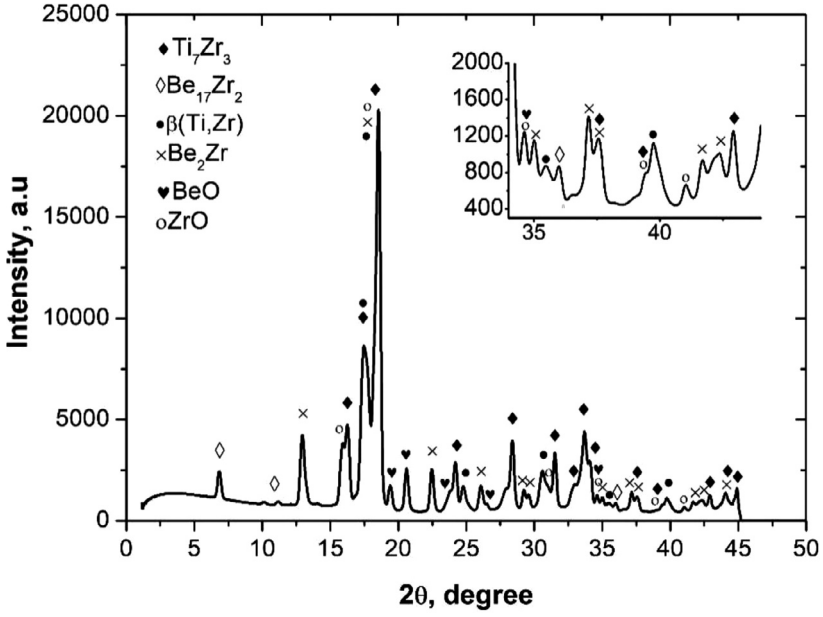

Fig. 1. Synchrotron XRD pattern of TiZr4Be brazing foil manufactured by melt spinning after annealing at 600°C for 2 h.

SEM images and EDS distribution maps of the W/TiZr4Be/Ta/TiZr4Be/Rusfer joint are presented in Fig. 2. Good interaction and formation of different phases promotes stronger binding of the materials. Microstructure of the Ta/W seam is different from those observed in [11] with identical brazing procedure. The only difference was the dimensions of the Ta layer, which was wider than base materials in [11]. In this work, the width of Ta and base materials were identical and mixing of melts at Rusfer/Ta and Ta/W seams was possible. Therefore, base materials can be dissolved in the melt during brazing and penetration of iron from Rusfer/Ta into Ta/W seam is observed. This could cause the shift of thermodynamical balance of the melt, which led to formation of different from [11] microstructure. The observed mixing of the melts could be expected in real manufacturing conditions, because usually a long brazing foil is used [27] and the amount of the melt of this foil is enough to wet the whole surface of a Ta interlayer (both with boundaries).

In spite of the difference at the Ta/W seam, the mechanical tests in this work provided results similar to [11]. The shear strength of the joints was measured to be 118±28 MPa and all joints failed at Rusfer/Ta interface that means the strength of the joint doesn't depend on Ta/W microstructure and the most brittle phase of the joint forms at the Rusfer/Ta interface. According to [27], this phase is Ta_2Be with needle-like shape.

3.2. Gas exposure

Fig. 3 shows experimental data on D_2 gas exposure of single components of the joint: W, Rusfer, Tantalum, and TiZr4Be brazing alloy. All materials have been exposed in one run for 50 hours at the D_2 pressure of 10^4 Pa that is far beyond operation conditions in fusion devices. Several experiments were performed at different temperatures in the range from 300 to 600°C. The Y axis is an average D concentration in materials assuming homogeneous distribution in the bulk.

The largest D retention was in the brazing alloy and Ta with the maximum at 600°C, although the H solubility decreases with the temperature in these materials. This indicates that the equilibrium D concentration was not achieved at 300°C and 400°C. A reduced absorption rate is usually caused by contamination of the surface and oxides were detected in the brazing layers by SynXRD.

The D retention in W and Rusfer was much smaller than in Ta and TiZr4Be, as it was expected from low H solubility in these materials.

Fig. 4 shows SynXRD patterns of the TiZr4Be foils after D_2 gas exposure. The phases are marked according to the ICDD PDF4+ database. Hydrides were not identified in the foils exposed at 300°C and 400°C and this correlates with a relatively low deuterium retention (fig. 3) in these conditions. Oxides were not detected also that indicates the reduction of their amount in hydrogen environment. Additionally, $Be_{17}Zr_2$ and β(Ti,Zr) dissolved, likely, because of long annealing time during exposure (50 hours).

Hydrides formed in the foils exposed to 500°C and 600°C. In the pattern of the foil exposed to 500°C, one can see titanium deuteride ($TiH_{1.96}$, ICDD # 04–002-5203) formation and no Ti-Zr phases. It means that all titanium interacted with deuterium leaving αZr solid solution. In the foil exposed to 600°C, intense peaks of $TiZrD_2$ ($TiZrD_2$, ICDD # 01-082-7060) and $Be_2ZrD_{0,56}$ ($Be_2ZrH_{0,56}$, ICDD # 04-013-0305) dominate with no clear peaks of intermetallic compounds. The presence of other phases is possible, but with lower concentrations.

Embrittlement of Ta and brazing alloys was also observed after high temperature gas exposure at 500 and 600 °C and this correlates well with hydrides formation observed by SynXRD (Fig. 4).

The next step was D_2 gas exposure of the full joints (Fig. 5, Table 1). The length of the steel part exceeded the tungsten part. This geometry was chosen for the possibility to perform mechanical tests after exposure. The first series was done at the same pressure of 10^4 Pa and two temperatures of 300 and 600°C, and the joints failed in both cases. At $p = 100$ Pa, the samples failed at 300°C, but survived at 600°C. At $p = 1$ Pa, the samples survived both at 300 and 600°C. Examples of the failed and survived samples are presented in Fig. 5 a and b correspondingly. The brazing alloy turned to dust in the case of the failure. The tantalum part remained solid, but became brittle also.

The shear strength and the D retention were measured for the samples remained intact after exposure; the results are presented in Table 1. The joint loses 30% of its strength after exposure. Nevertheless, its strength is higher than that of diffusion bonded W/Ti/(91 grade steel) after D_2 exposure [28].

In contrast to preliminary experiments with single materials, the D retention is high not only after high temperature expo-

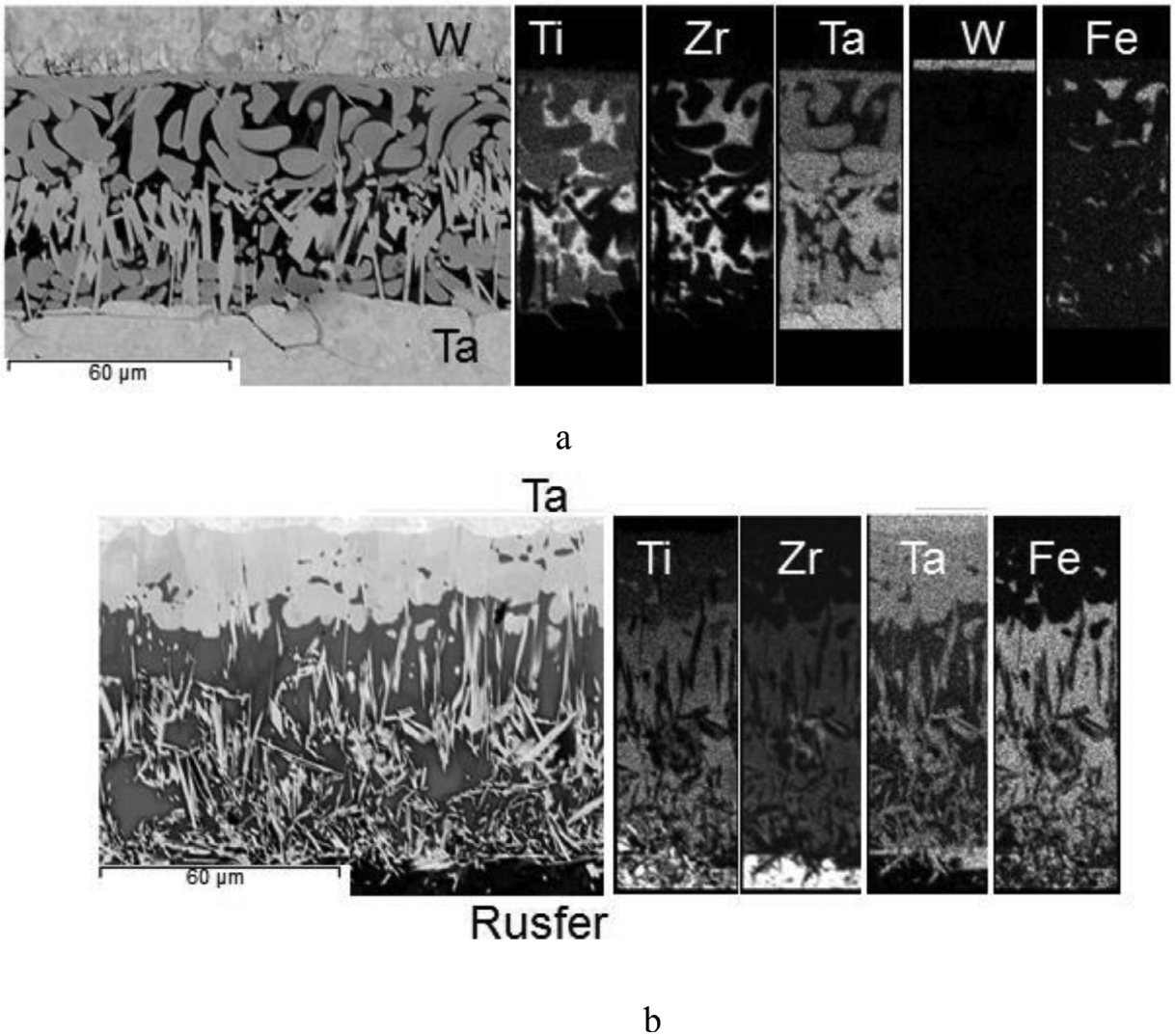

Fig. 2. SEM image with EDS maps of W/Ta/Rusfer joint brazed by TiZr4Be alloy: a) W/Ta seam; b) Ta/Rusfer seam.

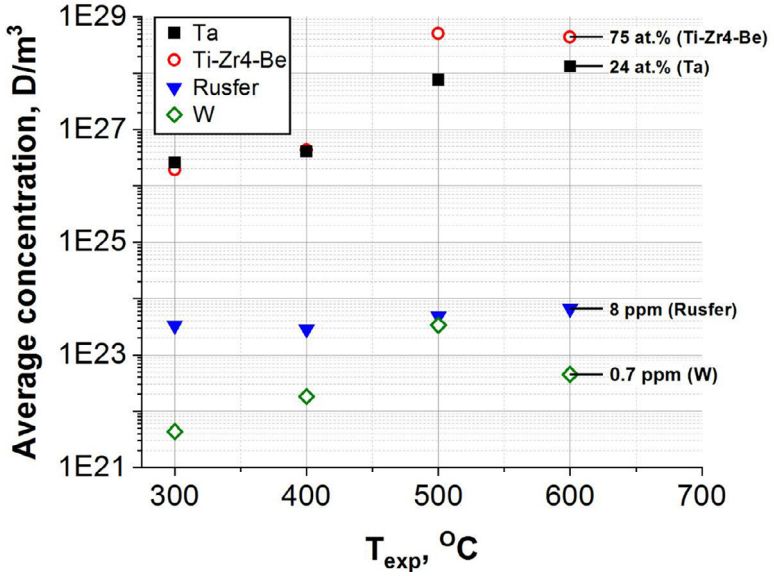

Fig. 3. The average D concentration in single materials (W, Ta, Rusfer, brazing alloy TiZr4Be) of the joint after exposure in D_2 gas at 10^4 Pa for 50 hours at different temperatures. The D concentration in atomic percent is indicated for several points as a reference.

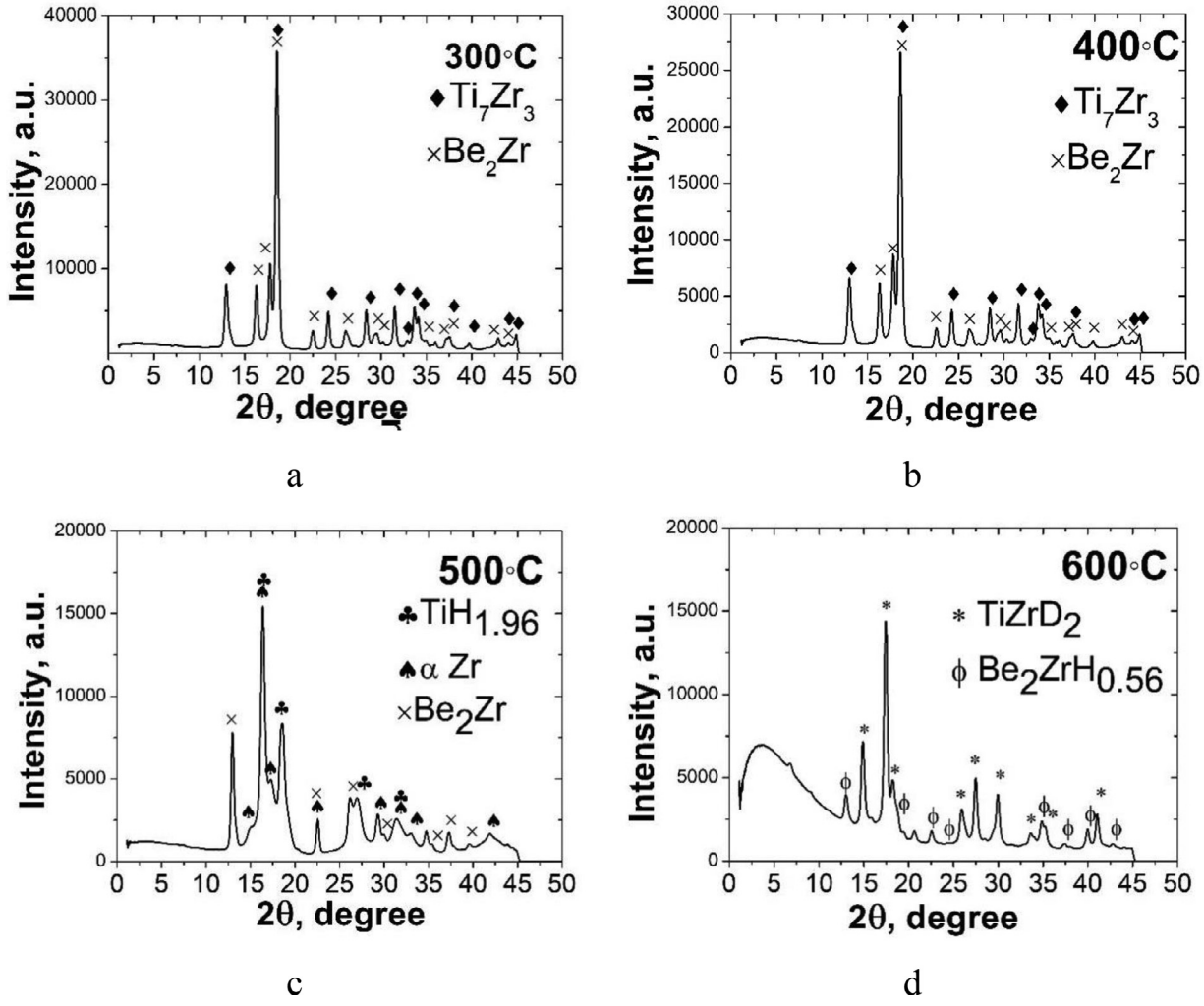

Fig. 4. Synchrotron XRD pattern of the TiZr4Be brazing foil manufactured by melt spinning after annealing at 600 °C for 2 h and D2 gas exposure for 50 h at different temperatures: a) 300 °C, b) 400 °C; c) 500 °C; d) 600 °C

Fig. 5. Photos of the joints: a) after 300°C, 100 Pa. b) after 600°C, 100 Pa.

sure, but also after exposure at 300°C. It decreases with the exposure temperature as it is expected for Ta and the brazing alloy in the equilibrium. Thus, D penetration into the brazing alloy and Ta was even better than in the case of single materials exposure that is possibly due to thermal treatment and suppression of surface oxidation. The sum of the D retention after separate exposure of the joint components is also provided in Table 1 for comparison. At 600°C, one can roughly estimate the pressure dependence of the D retention and it is close to the square root as expected from the Siverts law. Gas absorption measurements were available only in few experiments and can be compared with TDS only in one experiment. A lower D amount in TDS could be

Table 1
The shear strength of the W/TiZr4Be/Ta/TiZr4Be/Rusfer brazed joint, the D retention, and the average D concentration (assuming all D atoms are trapped in the joining layer) after deuterium gas exposure.

T,°C	P, Pa	Shear strength, MPa	D retention, 10^{22} D/m^{2}TDS data	D/Me, at. %TDS data	Gas absorption, 10^{22} D/m^2
As-produced		118±28			
300 (Separate exposure)	10000	-	6.1±1.2	0.32±0.06	-
600 (Separate exposure)	10000	-	550±50	31±6	-
300	10000	failure	-	-	-
600	10000	failure	-	-	-
300	100	failure	-	-	230±50
600	100	86±27	30±6	1.65±0.35	47±10
300	1	80±16	20±4	1.1±0.2	-
600	1	80±30	2.8±0.5	0.16±0.03	-
600 (5 h in plasma facility)	1	-	2.3±0.4	0.13±0.03	-

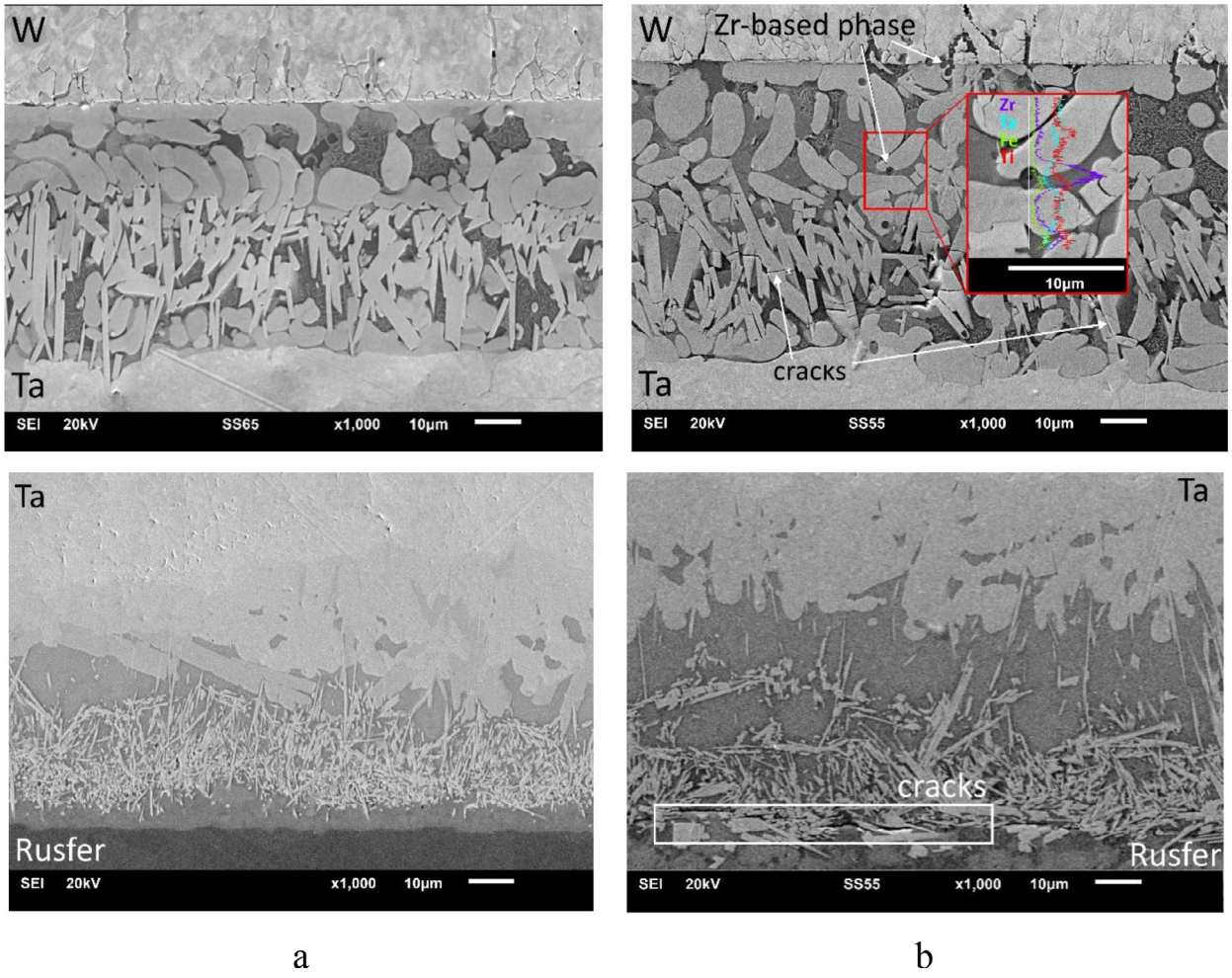

Fig. 6. The SEM image of W/Ta/Rusfer joint brazed by TiZr4Be alloy: a) after annealing at 600°C for 100 h; b) after exposure in 100 Pa D_2 gas at 600°C for 50 h.

due to partial D release during the storage and shear strength tests.

There is a clear correlation between the D concentration in the samples and their destruction. Formation of brittle hydride phases in the case of the high D concentration is confirmed by SynXRD (Fig. 4), and this should be the key mechanism of material destruction. In the case of the D concentration of few atomic percent and less, the joints have acceptable mechanical properties. This is the case for 600°C at 1 and 100 Pa, and for 300°C and 1 Pa.

Fig. 6 shows cross sections of the joints after 100 h annealing at 600°C and after 100 Pa D_2, 600°C for 50 h, a and b correspondingly. There is no microstructural degradation after pure annealing at 600°C (Fig. 6a) and no changes are expected after pure annealing at 300°C as well. However, some cracks were formed in Ta_2Be phase both in W/Ta and Ta/Rusfer seams in the joints exposed to D_2 gas. A new phase with a round outline is observed also in the W/Ta seam (Fig. 6b), where EDS detected prevail of Zr. This Zr-based phase is suggested to be a zirconium based hydride, since it is observed only in deuterium exposed samples. This could be the beryllium-zirconium hydride, since it was detected after exposure of the single brazing alloy (Fig. 4).

One should mention that cracks were not distributed homogeneously in the brazed layer. Fig. 6b corresponds to the area close to the side surface of the joint. Deeply in the bulk, there were still Zr-based round-shape phases in the W/Ta seam, but no cracks in both seams. It is suggested that deuterium absorption goes pre-

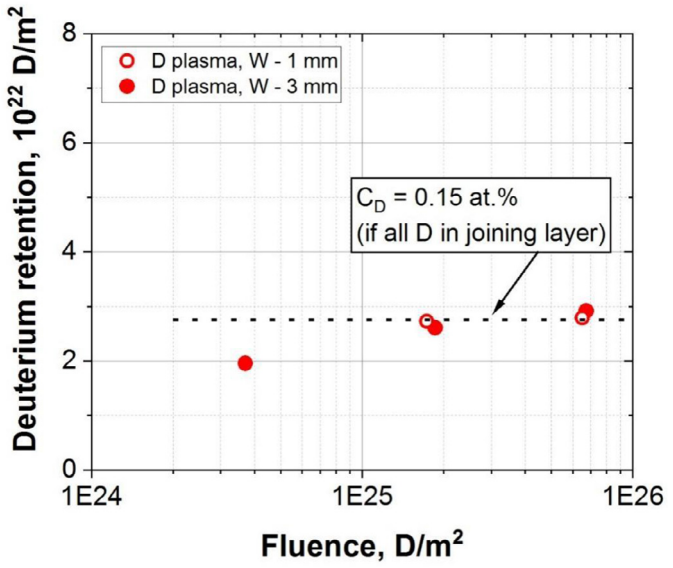

Fig. 7. The fluence dependence of the D retention in W/TiZr4Be/Ta/TiZr4Be/Rusfer brazed joints after plasma irradiation. The dashed line corresponds to C_D=0.15 at.% in assumption of D presence only in the brazing layer similar to the data in Table 1.

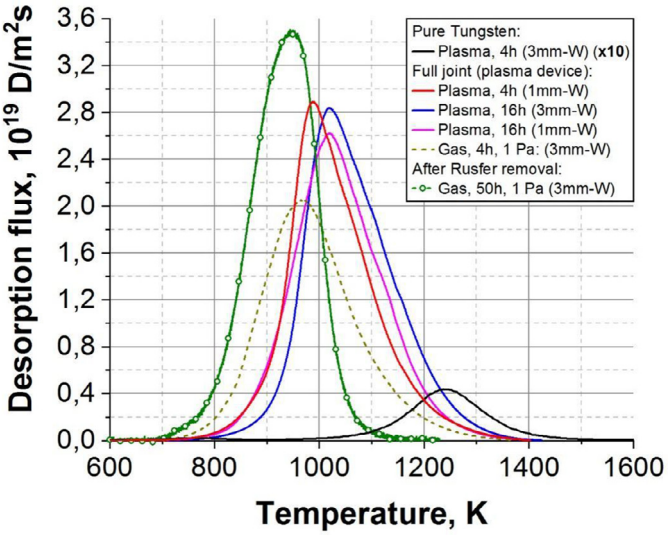

Fig. 8. Typical TDS spectra of D_2 desorption after deuterium gas or plasma exposure at 600°C. The amplitude of the TDS spectrum for pure W is multiplied by 10 times.

dominantly at side surfaces leading to a higher D concentration in the edges of brazed seams and higher embrittlement.

3.3. Plasma exposure

To analyse the rate of D accumulation in the joints in plasma environment, a series of plasma irradiations was performed with the ion incident flux comparable to the value expected at the DEMO first wall. The main set of experiments was done with the standard 3 mm thick W layer. In addition, a part of experiments was done with the 1 mm thick W layer for comparison. The irradiation time was varied from 2 to 16 hours with the same flux of about 1.2 $\times$ 10^{21} D/m^{2}s. All samples successfully survived after all plasma experiments.

The D transport through W is strongly affected by presence of lattice defects. The concentration of trapping sites depends strongly on the grade of material. In particular, the effective diffusivity in hot-rolled W foils can be lower by several orders of magnitude in comparison to theoretical values [29]. In this work, the D retention in the joints was substantial already after 2 hours of plasma exposure and exceeded the D retention after similar exposure of the W part only (without steel and brazing layers) by at least 30 times. It was suggested, therefore, that deuterium can penetrate through W quickly to the brazing layer. However, we found later that dependences on the fluence and on the thickness of W layers are very weak (fig. 7). Only the number for the smallest fluence is slightly less than other data points. The total D retention in these experiments is close to the number measured in gas exposure experiments in similar conditions (1 Pa, 600°C). Therefore, it was concluded that the main source of D in the samples in our experiments was not the plasma, but surrounding D_2 gas itself. For verification, a gas exposure experiment without plasma irradiation has been done inside the plasma facility and the D retention was again nearly at the same level (C_D=0.13 at.% after 5 hours D_2 exposure).

Fig. 8 collects several TDS spectra for deuterium gas and plasma exposure at 600°C. The heating rate in these experiments was 0.2 K/s. The D release from pure W after plasma exposure occurs at highest temperatures, but the total deuterium retention is very small as mentioned before. In spite of the similar total D retention in other experiments, there are some differences in the dynamics of D release caused partly by a different way of sample preparation for TDS. In the case of plasma exposure, the whole joints were heated (solid lines) and there is a minor difference in TDS spectra for the joints. Deuterium desorption starts around 800 K and has a maximum at about 1000 K. A small shift to higher temperatures is observed with the increase of the irradiation time and the thickness of the W layer due to a longer diffusion path for deuterium atoms. In spite of the similar D retention in the joints after gas and plasma exposure, the TDS spectrum is slightly different. The D release in the gas exposed sample starts earlier and the TDS peak is broader, however, the reason of this difference is presently unclear.

The last spectrum corresponds to gas exposure experiments performed at the same pressure, but after longer exposure time and after mechanical tests. Therefore, two pieces (W/Ta and Rusfer) were heated separately. The D amount in the Rusfer part was very small and the spectrum in the Fig. 8 is for the part consisting of W, Ta, and the alloy. Again, we see a shift of D release to lower temperatures, since D can escape from Ta directly to vacuum without diffusion through the base materials. From this spectrum, one can suggest that long time baking at 750-800 K should be enough for hydrogen isotope removal from W-Rusfer joints.

Finally, one can conclude that the chosen brazing technique can provide a PFC compatible with DEMO operation conditions, but care must be taken in the case of appearance of elevated pressures of H isotopes.

4. Summary

New challenges appear in development of PFCs for future DEMO reactors, such as safe joining of tungsten to RAFM steels. W-Rusfer joints have been produced using the fully reduced activation brazing alloy TiZr4Be and the Ta interlayer (W/TiZr4Be/Ta/TiZr4Be/Rusfer) and demonstrated good mechanical properties. The phase composition of the brazing alloy was determined by synchrotron XRD, it mainly consists of Ti_7Zr_3, $Be_{17}Zr_2$, β(Ti,Zr) solid solution and Be_2Zr. The shear strength of the as-joined composition is 118±28 MPa.

Single materials and prepared W-Rusfer joints were exposed in D_2 gas. Large D accumulation and destruction of the brazing alloy was observed after long time exposure at high pressures (10^4 Pa) and temperatures in the range of 300-600°C. Destruction of the material correlated with formation of hydrides detected by syn-

chrotron XRD. The acceptable D accumulation without failure of the joints was at (T> 300°C and P<1 Pa) typical for normal operation of plasma facing components at the DEMO first wall, and even at higher pressures (≤100Pa) for temperatures T ≥ 600°C.

W-Rusfer joints were also exposed to D plasma at 600°C. The D retention was very close to gas exposure experiments at the same pressure of the working gas and there was a weak dependence on the fluence and the thickness of the W.

Thus, hydrogen isotope retention in materials may limit the choice of possible solutions for PFC. In particular, the chosen brazing technique requires careful operation at elevated pressures of H isotopes.

Credit statement

Y. Gasparyan - Conceptualization, Supervision, Writing - Original Draft, D. Bachurina - Investigation, Writing - Original Draft, V. Efimov - Investigation, Data Curation, J. Gurova - Investigation, F. Podolyako - Investigation, N. Sergeev - Investigation, Writing - Review & Editing, I. Sorokin - Methodology, Investigation, A. Suchkov - Conceptualization, Methodology, Writing - Review & Editing, N. Bobyr - Investigation, Writing - Review & Editing, I. Kozlov - Investigation, E. Kulikova - Data Curation, A. Spitsyn - Methodology, Writing - Review & Editing,

Declaration of Competing Interest

The authors declare that they have no known competing financial interests or personal relationships that could have appeared to influence the work reported in this paper.

Acknowledgments

The work was supported by the Russian Science Foundation project № 17-72-20191. Sample characterization using the Synchrotron was done with the support of the Ministry of Science and Higher Education of the Russian Federation (Agreement No. 075-15-2021-1352).

References

[1] V.M. Chernov, M.V Leontyeva-Smirnova, D.A. Blokhin, A.G. Ioltukhovsky, E.M. Mozhanov, A.B. Sivak, Heat-resistant ferritic-martensitic steel RUSFER-EK-181 (Fe-12Cr-2W-V-Ta-B) for fusion power reactor, Int. Atomic Energy Agency (IAEA) (2010) http://www-pub.iaea.org/MTCD/Meetings/PDFplus/2010/cn180/cn180_BookOfAbstracts.pdf.

[2] H. Tanigawa, E. Gaganidze, T. Hirose, M. Ando, S.J. Zinkle, R. Lindau, E. Diegele, Development of benchmark reduced activation ferritic/martensitic steels for fusion energy applications, Nucl. Fusion. 57 (2017) 92004, doi:10.1088/1741-4326/57/9/092004.

[3] G. Pintsuk, Tungsten as a Plasma-Facing Material, Elsevier Inc., 2012, doi:10.1016/B978-0-08-056033-5.00118-X.

[4] E. Martelli, G. Caruso, F. Giannetti, A. Del Nevo, Thermo-hydraulic analysis of EU DEMO WCLL breeding blanket, Fusion Eng. Des. 130 (2018) 48–55, doi:10.1016/j.fusengdes.2018.03.030.

[5] J. Aubert, G. Aiello, R. Boullon, F.A. Hernández, J.C. Jaboulay, DEMO breeding blanket helium cooled first wall design investigation to cope high heat loads, Fusion Eng. Des. (2019) 0–1, doi:10.1016/j.fusengdes.2019.01.009.

[6] W.W. Basuki, R. Dahm, J. Aktaa, Thermomechanical analysis of diffusion-bonded tungsten/EUROFER97 with a vanadium interlayer, J. Nucl. Mater. 455 (2014) 635–639, doi:10.1016/j.jnucmat.2014.09.007.

[7] Q. Cai, W. Zhu, Y. Ma, W. Liu, X. Pang, C. Liang, Rational design of composite interlayer for diffusion bonding of tungsten–steel joints, Int. J. Refract. Met. Hard Mater. 70 (2018) 155–161, doi:10.1016/j.ijrmhm.2017.10.002.

[8] D.D. Qu, M. Wirtz, J. Linke, R. Vaßen, J. Aktaa, Thermo-mechanical response of FG tungsten/EUROFER multilayer under high thermal loads, J. Nucl. Mater. 519 (2019) 137–144, doi:10.1016/j.jnucmat.2019.03.019.

[9] S. Heuer, T. Lienig, A. Mohr, T. Weber, G. Pintsuk, J.W. Coenen, F. Gormann, W. Theisen, C. Linsmeier, Ultra-fast sintered functionally graded Fe/W composites for the first wall of future fusion reactors, Compos. Part B Eng. 164 (2019) 205–214, doi:10.1016/j.compositesb.2018.11.078.

[10] D. Bachurina, V. Vorkel, A. Suchkov, J. Gurova, A. Ivannikov, M. Penyaz, I. Fedotov, O. Sevryukov, B. Kalin, Overview of the mechanical properties of tungsten/steel brazed joints for the demo fusion reactor, Metals (Basel) 11 (2021) 1–11, doi:10.3390/met11020209.

[11] D. Bachurina, A. Suchkov, J. Gurova, V. Kliucharev, V. Vorkel, M. Savelyev, P. Somov, O. Sevryukov, Brazing tungsten/tantalum/RAFM steel joint for DEMO by fully reduced activation brazing alloy 48Ti-48Zr-4Be, Metals (Basel) 11 (2021), doi:10.3390/met11091417.

[12] V.M. Chernov, M.V. Leonteva-Smirnova, M.M. Potapenko, N.I. Budylkin, Y.N. Devyatko, A.G. Ioltoukhovskiy, E.G. Mironova, A.K. Shikov, A.B. Sivak, G.N. Yermolaev, A.N. Kalashnikov, B.V. Kuteev, A.I. Blokhin, N.I. Loginov, V.A. Romanov, V.A. Belyakov, I.R. Kirillov, T.M. Bulanova, V.N. Golovanov, V.K. Shamardin, Y.S. Strebkov, A.N. Tyumentsev, B.K. Kardashev, O.V. Mishin, B.A. Vasiliev, Structural materials for fusion power reactors - The RF R&D activities, Nucl. Fusion. 47 (2007) 839–848, doi:10.1088/0029-5515/47/8/015.

[13] V.M. Chernov, M.V. Leont'eva-Smirnova, E.M. Mozhanov, N.S. Nikolaeva, A.N. Tyumentsev, N.A. Polekhina, I.Y. Litovchenko, E.G. Astafurova, Thermal stability of the microstructure of 12% chromium ferritic–martensitic steels after long-term aging at high temperatures, Tech. Phys. 61 (2016) 209–214, doi:10.1134/S1063784216020092.

[14] V.T. Fedotov, A.N. Suchkov, B.A. Kalin, O.N. Sevryukov, A.A. Ivannikov, Stemet solders for brazing of modern technology materials, Tsvetnye Met (2014) 32–37.

[15] I.V. Fedotov, A.N. Suchkov, V.T. Fedotov, O.N. Sevryukov, B.A. Kalin, A.A. Ivannikov, Brazing of hexagonal boron-nitride ceramics with VT1-0 titanium alloy using a rapidly quenched titanium-based brazing alloy, Weld. Int. 29 (2015) 222–226, doi:10.1080/09507116.2014.911424.

[16] D. Bachurina, X.-Y. Tan, F. Klein, A. Suchkov, A. Litnovsky, J. Schmitz, J. Gonzalez-Julian, M. Bram, J.W. Coenen, Y.-C. Wu, C. Linsmeier, in: Self-Passivating Smart Tungsten Alloys for DEMO: a Progress in Joining and Upscale for a First Wall Mockup, Tungsten, 3, 2021, pp. 101–115, doi:10.1007/s42864-021-00079-5.

[17] R.D. Svetogorov, High-resolution powder diffraction at the XSA beamline of the Kurchatov Synchrotron Radiation Source, Conf. Proc. IX Natl. Cryst. Chem. Conf. (2018) 81.

[18] D. Bachurina, A. Suchkov, J. Gurova, M. Savelyev, P. Dzhumaev, I. Kozlov, R. Svetogorov, M. Leont'eva-Smirnova, O. Sevryukov, Joining tungsten with steel for DEMO: Simultaneous brazing by Cu-Ti amorphous foils and heat treatment, Fusion Eng. Des. 162 (2020) 112099, doi:10.1016/j.fusengdes.2020.112099.

[19] I. Fedotov, A. Suchkov, A. Sliva, P. Dzhumaev, I. Kozlov, R. Svetogorov, D. Bachurina, O. Sevryukov, Study of the microstructure and thermomechanical properties of Mo /graphite joint brazed with Ti – Zr – Nb – Be powder filler metal, J. Mater. Sci. 56 (2021) 11557–11568, doi:10.1007/s10853-021-06015-9.

[20] M.V. Leontiev-Smirnova, A.N. Agafonov, G.N. Ermolaev, A.G. Ioltukhovsky, E.M. Mozhanov, L.I. Reviznikov, V.V. Tsvelev, V.M. Chernov, T.M. Bulanova, V.N. Golovanov, Z.O. Ostrovsky, V.K. Shamardin, A.I. Blokhin, M.B. Ivanov, E.V. Kozlov, Yu.R. Kolobov, B.K. Kardashev, Microstructure and mechanical properties of low-activated ferritic-martensitic steel EK-181 (RUSFER-EK-181), Perspect. Mater. 6 (2006) 40–52 (*In Russian*).

[21] D. Bachurina, A. Suchkov, A. Filimonov, I. Fedotov, M. Savelyev, O. Sevryukov, B. Kalin, High-temperature brazing of tungsten with steel by Cu-based ribbon brazing alloys for DEMO, Fusion Eng. Des. (2019) 146, doi:10.1016/j.fusengdes.2019.02.072.

[22] R. Wenninger, R. Albanese, R. Ambrosino, F. Arbeiter, J. Aubert, C. Bachmann, L. Barbato, T. Barrett, M. Beckers, W. Biel, L. Boccaccini, D. Carralero, D. Coster, T. Eich, A. Fasoli, G. Federici, M. Firdaouss, J. Graves, J. Horacek, M. Kovari, S. Lanthaler, V. Loschiavo, C. Lowry, H. Lux, G. Maddaluno, F. Maviglia, R. Mitteau, R. Neu, D. Pfefferle, K. Schmid, M. Siccinio, B. Sieglin, C. Silva, A. Snicker, F. Subba, J. Varje, H. Zohm, The DEMO wall load challenge, Nucl. Fusion. 57 (2017) 46002, doi:10.1088/1741-4326/aa4fb4.

[23] Y. Huang, F. Cismondi, E. Diegele, G. Federici, A. Del, F. Moro, N. Ghoniem, Thermo-structural design of the European DEMO water-cooled blanket with a multiscale-multiphysics framework, Fusion Eng. Des. 135 (2018) 31–41, doi:10.1016/j.fusengdes.2018.07.007.

[24] R. Behrisch, G. Federici, A. Kukushkin, D. Reiter, Material erosion at the vessel walls of future fusion devices, J. Nucl. Mater. 313–316 (2003) 388–392, doi:10.1016/S0022-3115(02)01580-5.

[25] N.S. Sergeev, I.A. Sorokin, Modification of the tungsten surface under the beam plasma discharge plasmas, in: 47th EPS Conf. Plasma Physics47th EPS Conf. Plasma Phys, 2021, pp. 197–200.

[26] M.M. Codescu, A. Vladescu, V. Geanta, I. Voiculescu, I. Pana, M. Dinu, A.E. Kiss, V. Braic, D. Patroi, V.E. Marinescu, Zn based hydroxyapatite based coatings deposited on a novel FeMoTaTiZr high entropy alloy used for bone implants, Surfaces and Interfaces. (2021) 101591. https://doi.org/10.1016/j.surfin.2021.101591.

[27] A. Gervash, R. Giniyatulin, T. Guryeva, D. Glazunov, V. Kuznetsov, I. Mazul, P.Piskarev Ogursky, V. Safronov, R. Eaton, R. Raffray, O. Sevryukov, The development of technology of Be/CuCrZr joining using induction brazing, Fusion Eng. Des. 146 (2019) 2292–2296, doi:10.1016/j.fusengdes.2019.03.175.

[28] J. Wang, J. Huang, H. Sun, X. Gao, W. Wang, Q. Li, C. Xie, X. Wang, Z. Chen, Q. Gao, S. Liu, G. Luo, E ff ect of deuterium on bonding quality of W /Ti / Steel HIP joints in fi rst wall application, Fusion Eng. Des. 138 (2019) 313–320, doi:10.1016/j.fusengdes.2018.12.010.

[29] Y. Gasparyan, M. Rasinski, M. Mayer, A. Pisarev, J. Roth, Deuterium ion-driven permeation and bulk retention in tungsten, J. Nucl. Mater. 417 (2011) 540–544, doi:10.1016/J.JNUCMAT.2010.12.119.